The Journal of Immunology

Dendritic Cell Accumulation in the Gut and Central Nervous System Is Differentially Dependent on α4 Integrins

Christopher Sie, Laura Garcia Perez, Mario Kreutzfeldt, Maria Potthast, Caspar Ohnmacht, Doron Merkler, Samuel Huber, Anne Krug and Thomas Korn

J Immunol 2019; 203:1417-1427; Prepublished online 9 August 2019;
doi: 10.4049/jimmunol.1900468
http://www.jimmunol.org/content/203/6/1417

The Journal of Immunology is published twice each month by
The American Association of Immunologists, Inc.,
1451 Rockville Pike, Suite 650, Rockville, MD 20852

Print ISSN: 0022-1767 Online ISSN: 1550-6606.

Dendritic Cell Accumulation in the Gut and Central Nervous System Is Differentially Dependent on α4 Integrins

Christopher Sie,*,† Laura Garcia Perez,‡ Mario Kreutzfeldt,§ Maria Potthast,¶ Caspar Ohnmacht,¶ Doron Merkler,§ Samuel Huber,‡ Anne Krug,‖ and Thomas Korn*,†,#

Homing of pathogenic CD4$^+$ T cells to the CNS is dependent on α4 integrins. However, it is uncertain whether α4 integrins are also required for the migration of dendritic cell (DC) subsets, which sample Ags from nonlymphoid tissues to present it to T cells. In this study, after genetic ablation of *Itga4* in DCs and monocytes in mice via the promoters of *Cd11c* and *Lyz2* (also known as LysM), respectively, the recruitment of α4 integrin–deficient conventional and plasmacytoid DCs to the CNS was unaffected, whereas α4 integrin–deficient, monocyte-derived DCs accumulated less efficiently in the CNS during experimental autoimmune encephalomyelitis in a competitive setting than their wild-type counterparts. In a noncompetitive setting, α4 integrin deficiency on monocyte-derived DCs was fully compensated. In contrast, in small intestine and colon, the fraction of α4 integrin–deficient CD11b$^+$CD103$^+$ DCs was selectively reduced in steady-state. Yet, T cell–mediated inflammation and host defense against *Citrobacter rodentium* were not impaired in the absence of α4 integrins on DCs. Thus, inflammatory conditions can promote an environment that is indifferent to α4 integrin expression by DCs. *The Journal of Immunology*, **2019, 203: 1417–1427.**

CD11c$^+$ myeloid cells are present in the noninflamed CNS. Both juxtavascular and intraparenchymal localization of CD11c$^+$ cells have been demonstrated in the CNS in steady-state (1, 2). Although perivascular MHC class II (MHC-II)–expressing cells were initially termed "perivascular microglia" (3), it is now clear that they are distinct from proper intraparenchymal microglial cells (4–6). Whereas intraparenchymal CD11c$^+$ cells are likely microglial cells that are dispensable for the presentation of Ags to T cells, perivascular CD11c$^+$ cells are of hematopoietic origin and serve a nonredundant role for the stimulation of T cells in the CNS in steady-state and during inflammation (7–10).

A series of recent studies have addressed the provenance and maintenance of perivascular and meningeal CD11c$^+$ cells within the CNS compartment (10–12). Similarly as in T cells, integrin expression in dendritic cells (DCs) has been proposed to mediate firm adhesion of DCs to CNS endothelial cells as a prerequisite for their transmigration into the CNS compartment. Whereas, in some studies, α4β1 integrin (VLA-4) was found to mediate DC adhesion to endothelial cells (13), other reports stressed the importance of αLβ2 integrin (LFA-1) in transmigration of DCs across the inflamed endothelial barrier (14). In addition, it appears that pre–conventional DCs (cDCs) migrate to the meningeal and perivascular compartment in steady-state, become mature DCs, and stay in situ with a $t_{1/2}$ of 5–7 d (15).

Limited information exists as to the fraction of plasmacytoid DCs (pDCs) and cDCs within the CNS DC compartment. In particular, pDCs were regarded as gate keepers of immunologic homeostasis because of their potential tolerogenic functions (16). Immature pDCs were even considered for adoptive immune therapeutic approaches to reinstall immune homeostasis in autoimmune neuroinflammation (17). Yet, given their role as primary sources of type I IFNs in response to foreign DNA stimulation, the role of pDCs in priming and maintaining encephalitogenic T cell responses is controversial and both proinflammatory functions of pDCs as well as tolerizing functions of pDCs were reported. Whereas anti–PDCA-1 mediated depletion of pDCs prior to immunization decreased experimental autoimmune encephalomyelitis (EAE), delayed ablation of pDCs exacerbated the disease course (18). The mechanism how pDCs induce tolerance is elusive, and various mechanisms including selective expansion of Foxp3$^+$ regulatory T (Treg) cells in an Ag-specific manner have been discussed (16). The functional diversity of cDCs is only beginning to be understood (19). A recent concept proposed that distinct subsets of cDCs induce distinct phenotypes of T cell responses (20). For example, in the gut lamina propria, CD11b$^+$CD103$^-$ and

*Abteilung für Experimentelle Neuroimmunologie, Klinikum rechts der Isar, Technische Universität München, 81675 Munich, Germany; †Klinik für Neurologie, Klinikum rechts der Isar, Technische Universität München, 81675 Munich, Germany; ‡I. Medizinische Klinik und Poliklinik, Universitätsklinikum Hamburg-Eppendorf, 20246 Hamburg, Germany; §Division of Clinical Pathology, Department of Pathology and Immunology, University of Geneva, 1211 Geneva, Switzerland; ¶Center of Allergy and Environment, Helmholtz Center and Technical University of Munich, 80802 Munich, Germany; ‖Institute for Immunology, Biomedical Center, Ludwig Maximilians University of Munich, 82152 Planegg-Martinsried, Germany; and #Munich Cluster for Systems Neurology, SyNergy, 81377 Munich, Germany

ORCIDs: 0000-0002-8066-7539 (C.S.); 0000-0003-0335-2733 (M.K.); 0000-0001-7933-9426 (M.P.); 0000-0002-3633-0955 (T.K.).

Received for publication April 24, 2019. Accepted for publication July 13, 2019.

This work was supported by a Ph.D. fellowship from the Boehringer Ingelheim Fonds (to C.S.). C.O. is supported by the European Research Council (ERC) (StgG 716718), by the Deutsche Forschungsgemeinschaft (SFB 1371-P07 and within FOR2599), and by an intramural fund of the Helmholtz Zentrum Muenchen. T.K. is supported by the Deutsche Forschungsgemeinschaft (SFB1054-B06, TRR128, and SyNergy), the German Federal Ministry of Education and Research (T-B in NMO), and the ERC (CoG 647215).

C.S. performed most experiments, analyzed data, and interpreted results; L.G.P. and S.H. performed *Citrobacter rodentium* infection experiments and analyzed data; M.K. and D.M. analyzed histologic data; M.P. and C.O. performed and analyzed some lamina propria stainings; A.K. designed experiments and interpreted results; and T.K. conceived and initiated the study, interpreted results, and wrote the paper.

Address correspondence and reprint requests to Dr. Thomas Korn, Klinikum rechts der Isar, Technische Universität München, Ismaninger Strasse 22, 81675 Munich, Germany. E-mail address: thomas.korn@tum.de

The online version of this article contains supplemental material.

Abbreviations used in this article: cDC, conventional DC; DC, dendritic cell; EAE, experimental autoimmune encephalomyelitis; KO, knockout; MHC-II, MHC class II; moDC, monocyte-derived DC; pDC, plasmacytoid DC; pTreg, peripherally induced Treg; Treg, regulatory T; WT, wild-type.

$CD11b^+CD103^+$ DCs (cDC2s) promote Th17 responses (21), whereas $CD11b^{low}CD103^+$ DCs induce Th1 responses and are particularly proficient in cross-presenting exogenous Ags to $CD8^+$ T cells (22–24).

Because the cerebrospinal fluid and CNS parenchyma were depleted of DCs in multiple sclerosis patients receiving a blocking Ab to α4 integrins, VLA-4 has been believed to control the access of DCs to the CNS compartment under inflammatory conditions in humans as well. The depletion of the CNS APC compartment due to administration of an anti–VLA-4 Ab (natalizumab) has also been blamed for the loss of immune surveillance and failure to control John Cunningham virus infection resulting in progressive multifocal leukoencephalopathy (25). After termination of natalizumab treatment, Ab desaturation of VLA-4 on immune cells takes ∼10 wk (26). Yet, the depletion of T cells in the cerebrospinal fluid compartment is prolonged until 6–12 mo after stopping natalizumab, suggesting that indirect effects such as the reduction of APCs in the cerebrospinal fluid space and the CNS parenchyma during and after natalizumab treatment might contribute to the delayed repletion of the cerebrospinal fluid space with T cells (27).

Using a genetic model, this study was designed to investigate the role of α4 integrins (encoded by *Itga4*) in DC subsets for populating the intracerebral APC niche during development, in homeostasis, and under inflammatory conditions. Complete ablation of *Itga4* both in pDCs and cDCs did not affect the overall Ag-presenting capacity of the CNS compartment in steady-state nor the accumulation of DCs in the CNS during inflammation. In the small intestinal lamina propria, the fraction of $CD11b^+$ cDC2s was significantly decreased in DC conditional α4 integrin–deficient mice in homeostasis. However, priming of protective Th17 responses was still sufficient in *Citrobacter rodentium* infection. We propose that α4 integrins on DCs do not directly control the trafficking of DCs into the CNS and are redundant for the recruitment of DCs into the gut lamina propria during inflammation.

Materials and Methods

Mice

The 2D2 MOG (35–55) TCR–specific transgenic mice (28) crossed with Foxp3-GFP knock-in mice (29) and $Itga4^{flox/flox}$ mice (30) have been previously described. CD11c Cre (31), CD11c-GFP Cre (32), and LysM Cre deleter strains (33) were obtained from The Jackson Laboratory. All mouse strains were on pure C57BL/6 genetic background. Mice were kept in specific pathogen-free conditions at the Technical University of Munich or the University Hospital Hamburg-Eppendorf in accordance with the local regulations for animal experimentation (Az ROB-55.2-2532.Vet_02-13-29 and ROB-55.2-2532.Vet_03-18-53, Bavarian State Authorities, Munich, Germany, and Az 28/14 "Behörde für Soziales, Familie, Gesundheit und Verbraucherschutz" Hamburg, Germany).

Induction of EAE

To induce EAE, mice were immunized s.c. (base of tail) with 200 μl of an emulsion containing 200 μg MOG (35–55) (MEVGWYRSPFSRVVHLYRNGK; Auspep, Tullamarine, Australia) and 500 μg *Mycobacterium tuberculosis* H37Ra (BD Difco) in CFA and received 200 ng PTX (Sigma-Aldrich) i.v. on the same day and 2 d after the immunization. Clinical signs of disease were monitored as described previously (34).

Adoptive transfer EAE

For adoptive transfer experiments, C57BL/6 wild-type (WT) donor mice were immunized with MOG (35–55) peptide in CFA and PTX according to the regimen for active induction of EAE. On day 7, draining lymph nodes and spleens were prepared, pooled, and ex vivo restimulated for 3 d with 35 μg/ml MOG (35–55) in the presence of TGF-β (0.25 ng/ml), IL-6 (5 ng/ml), IL-23 (6.5 ng/ml), and anti–IFN-γ (10 μg/ml) to skew Ag-specific T cells into Th17 cells. All cytokines were purchased from Miltenyi Biotec and R & D Systems. After isolation of $CD4^+$ T cells from the recall culture using Miltenyi Biotec untouched $CD4^+$ T cell purification beads, 6×10^6 $CD4^+$ T cells were transferred i.v. into recipient mice, concomitantly with i.p. injection of PTX on days 0 and 2 after adoptive transfer.

Expansion of DCs in vivo

B16 Flt3L–secreting melanoma cells were cultured and implanted as previously described (35). Briefly, cells were cultured in supplemented RPMI 1640 at 37˚C and 5% CO_2 for at least 3 d, subconfluently harvested, and s.c. injected in the neck at 6×10^6 cells in PBS per mouse. Mice were sacrificed after 7 d, and DCs were isolated as described below.

Generation of mixed bone marrow chimeras

Mice were irradiated at a dose of 11 Gy. A total of $10–20 \times 10^6$ donor bone marrow cells mixed 1:1 from CD45.1 wild-type donors and indicated knockout (KO) mice, depleted of $CD90.2^+$ cells using Miltenyi Microbeads, were injected i.v. into recipients within 16–20 h postirradiation. The reconstituted mice were maintained on antibiotic water (enrofloxacin, 0.1 mg/ml; Bayer) for 3 wk after transplantation. The reconstitution of the hematopoietic compartment was checked 5–6 wk after cell transfer in peripheral blood.

In vivo LFA-1 blockade

For in vivo blockade experiments, MOG (35–55)–immunized mice were treated with i.p. injections of anti–LFA-1 Ab (M17/4; Bio X Cell) or Rat IgG2a isotype control (clone 2A3; Bio X Cell) in PBS starting on day 5 (200 μg), followed by i.p. injections of 100 μg every other day until day 15 after immunization. Shortly after, mice were analyzed at peak disease.

Injection of anti-CD3 Ab

Mice were injected i.p. with 20 μg of anti-CD3e (clone 2C11; Bio X Cell) in PBS on days 0, 2, and 4 and weighed daily for a total of 7 d.

C. rodentium *infection*

Luciferase-expressing, nalidixic acid–resistant derivative of *C. rodentium* (ICC180) was grown overnight in lysogeny broth containing 50 μg/ml of nalidixic acid with shaking at 37˚C. Next day, the suspension of bacteria was washed twice with PBS, and the concentration was adjusted to 5×10^9 CFU/ml. Mice were infected by oral gavage with 0.2 ml of *C. rodentium* solution containing 1×10^9 CFU. On day 7 postinfection, mouse colon and cecum were dissected as described below, and fecal material was dissolved in PBS and seeded in serial dilutions on lysogeny broth agar plates with nalidixic acid for 24 h at 37˚C, followed by counting of colonies. These experiments were approved by the institutional review board "Behörde für Soziales, Familie, Gesundheit und Verbraucherschutz" (Hamburg, Germany).

Histology

Mice were perfused with cold PBS, followed by 4% paraformaldehyde fixation (pH 7.4). Brain and spinal cord were dissected and embedded in paraffin. Ag retrieval was performed on 3-μm thick sections according to standardized protocols by heating with citrate buffer (pH 6). Endogenous peroxidases (peroxidase blocking reagent; Dako) were neutralized and unspecific binding blocked for 5 min (PBS/1% BSA/2% FCS). For immunofluorescence, sections were blocked for 5 min (PBS/1% BSA/2% FCS) and subsequently incubated with monoclonal rat anti-GFP (clone FM264G; BioLegend). Bound Abs were visualized with Alexa Fluor 488–labeled goat anti-rat IgG (Thermo Fisher Scientific). Subsequently, sections were incubated with polyclonal rabbit anti-mouse CD3 (Dako) and visualized with Alexa Fluor 647–labeled donkey anti-rabbit secondary Ab. Immunostained sections were scanned using Pannoramic digital slide scanner 250 FLASH II (3DHISTECH) in 200× magnification.

Preparation of mononuclear cells

At the peak of disease, CNS-infiltrating cells were isolated after perfusion through the left cardiac ventricle with PBS. Brain and spinal cord were extracted and meningeal layers of the spinal cord stripped under microscopic dissection. Tissues were digested with collagenase D (2.5 mg/ml) and DNase I (1 mg/ml) at 37˚C for 45 min. After passing the tissue through a 70-μm cell strainer, cells of the spinal cord and brain were separated by discontinuous Percoll gradient (70%/37%) centrifugation. Mononuclear cells were isolated from the interphase.

Isolation of lamina propria mononuclear cells

Peritoneal cavity was opened, mesenteric lymph nodes were retrieved, and small and large intestines were dissected and cleaned with HBSS on ice.

Fat and Peyer patches (if applicable) were removed and intestinal contents flushed with HBSS. Intestines were cut into segments of 5 mm, washed in HBSS, and epithelial layers removed by shaking in HEPES-buffered HBSS containing 0.25 mM EDTA at 37°C for 30 min, followed by repetitive washing in HBSS. Cells were extracted by incubation with DNase I (0.2 mg/ml) and Liberase TL (0.17 mg/ml) at 37°C for 15 min, followed by inactivation using RPMI 1640 supplemented with 10% FCS. Suspension and remaining tissue were forced through a 100-μm cell strainer, washed in RPMI 1640, and subjected to 37% Percoll purification, with mononuclear cells being retrieved from the pellet. Mesenteric lymph nodes were digested with collagenase D (2.5 mg/ml) and DNase I (1 mg/ml) at 37°C for 30 min and passed through a 70-μm cell strainer.

In vivo proliferation of Ag-specific T cells

Lymph nodes and spleens from naive 2D2 × Foxp3-GFP mice were isolated, pre-enriched using Miltenyi Biotec CD4 (L3T4) purification beads, and sorted for $CD44^{-}Foxp3\ (GFP)^{-}$ cells on a MoFlo II cell sorter. Obtained cells were labeled using eBioscience Cell Proliferation Dye eFluor 450, and 3×10^6 labeled CD4 T lymphocytes were injected i.v. into recipient mice. Twenty four hours later, mice were immunized with MOG (35–55) peptide as described above. Cells were reisolated from draining axillary and inguinal lymph nodes 4 d after immunization, and dilution of proliferation dye was assessed by flow cytometry. Proliferation index was calculated with R version 3.5.3 (R Core Team, 2019) using the package flowFit version 1.20.1 (36).

Intracellular cytokine staining and flow cytometry

Cells were stained with LIVE/DEAD fixable dyes (Aqua [405 nm excitation], Invitrogen) and Abs to surface markers: CD3e (145-2C11), CD4 (GK1.5 or RM4-5), CD8a (53-6.7), CD11b (M1/70), CD11c (HL3), CD19 (1D3 or 6D5), CD44 (IM7), CD45 (30-F11), CD45.1 (A20), CD45.2 (104), CD45R (B220; RA3-6B2), CD49d (a4 integrin, 9C10/MFR.4.B), CD64 (X54-5/7.1), Thy1.1 (CD90.1, Ox-7), CD103 (2E7), CD115 (AFS98), CD135 (FLT3; A2F10), CD317 (BST-2; eBio927), CD172 (SIRPα, P84), 2D2 TCR Vα3.2 (RR3-16) and Vβ11 (RR3-15), F4/80 (BM8), Ly-6G (1A8), Ly-6C (HK1.4), MHC-II(M5/114.15.2), NK1.1 (PK136), Siglec-H (eBio440c), and XCR-1 (ZET); all BD Biosciences, eBioscience, or BioLegend. For intracellular cytokine staining, cells were restimulated with 50 ng/ml PMA (Sigma-Aldrich), 1 μg/ml ionomycin (Sigma-Aldrich), and monensin (1 μl/ml BD GolgiStop) at 37°C for 2.5 h. Subsequent to LIVE/DEAD and surface staining, cells were fixed and permeabilized (Cytofix/Cytoperm and Perm/Wash Buffer; BD Biosciences) and stained for cytokines IL-17A (TC11-18H10.1; BioLegend), IFN-γ (XMG1.2; eBioscience), and GM-CSF (MP1-22E9; BD Biosciences). Intranuclear stainings for Foxp3 (FJK-16s), IRF8 (V3GYWCH), RORγt (AFKJS-9), Gata3 (TWAJ), and Helios (22F6) were performed using the Transcription Factor Staining Set (eBioscience). Cells were analyzed using a CyAn ADP 9 Flow Cytometer (Beckman Coulter) and a CytoFlex S (Beckman Coulter). Cell counting was performed by a Guava easyCyte 5HT Cytometer (Merck Millipore) together with 7-AAD (BD Biosciences), Fixable Red Dead Cell Stain (Thermo Fisher Scientific), or Fixable Viability Dye eFluor 520 (eBioscience) and CD45 (30-F11) or CD45.2 (104). All data analysis was facilitated using FlowJo version 10 (Tree Star). For intravascular staining, mice were injected i.v. with 1 μg of CD45.2 (104) or CD45 (30-F11) in 200 μl PBS 5 min before sacrificing.

Quantification and statistical analysis

Statistical evaluations of cell frequency measurements and cell numbers were performed by one-way ANOVA, followed by Tukey multiple comparisons test when three genotypes of a single-cell population were compared; by one-way ANOVA, followed by Sidak multiple comparison test when two genotypes of multiple cell populations were compared; or by two-way ANOVA, followed by Sidak multiple comparisons test when three genotypes of multiple-cell populations were compared, as indicated in the figure legends. Ratios of mixed bone marrow chimerism were compared with the indicated reference population for any given organ using one-way ANOVA, followed by Dunnett multiple comparisons test. Multiplicity adjusted p values <0.05 were considered significant. Differences of same-day littermate analyses for the gut were evaluated using two-tailed, paired Student tests. EAE scores between groups were analyzed as disease burden per individual day with one-way ANOVA and Dunnett post hoc test. Body weight loss was assessed by two-way ANOVA, followed by Sidak multiple comparisons test. *Citrobacter* CFUs were compared using a two-tailed, unpaired Student t test. Survival curves were analyzed by log-rank (Mantel–Cox) test. Statistical analysis was performed in GraphPad Prism 8.1.0 (GraphPad Software).

Results

Genetic ablation of Itga4 in DCs has no effect on the DC niche in the CNS

To test whether genetic ablation of *Itga4* in $CD11c^{+}$ cells interfered with the establishment of a functional APC niche within the CNS, we crossed CD11c Cre (31) or CD11c-GFP Cre mice (32) with $Itga4^{flox/flox}$ mice (30) to generate DC conditional α4 integrin–deficient mice, termed $Itga4^{\Delta DC}$. The ablation of *Itga4* was highly efficient in $CD11c^{+}$ cells in the spleen in steady-state (Supplemental Fig. 1A), and even pre-cDC precursors in the bone marrow were efficiently ablated of α4 integrin expression (Supplemental Fig. 1B). The CD11c Cre deleter strain (31) is known to also affect non-DC immune cell populations to varying degrees across different floxed alleles (37, 38). Therefore, we tested for α4 integrin mosaics in lymphoid and myeloid populations of $Itga4^{\Delta DC}$ mice and confirmed this prior observation (Supplemental Fig. 1C). However, whereas *Itga4* ablation was complete in DCs, recombination was only partial in non-DC immune cell populations (Supplemental Fig. 1C).

In the CNS, the distribution of $CD11c^{+}$ cells in the meninges, plexus choroideus, and perivascular space was identical in $Itga4^{\Delta DC}$ and CD11c Cre x $Itga4^{flox/wt}$ control mice (Fig. 1A). Using a gating strategy with established markers (Fig. 1B), we identified within the $CD11c^{+}MHC\text{-}II^{+}$ gate, pDCs ($BST\text{-}2^{+}$), cDC1s ($CD11b^{-}CD103^{+}$), and cDC2s ($CD11b^{+}CD103^{-}$) in the CNS in steady-state (Fig. 1B) and in "elevated homeostasis" after Flt3L treatment, which expands $CD11c^{+}$ cells in vivo under noninflammatory conditions (15) (Supplemental Fig. 1D). These data suggested that the expression of α4 integrins on $CD11c^{+}$ cells was dispensable for the recruitment and maintenance of DCs or $CD11c^{+}MHC\text{-}II^{-}$ DC precursor cells into the CNS niche in steady-state.

To test whether α4 integrin expression on DCs was required for their presence in the CNS in a competitive setting, mixed bone marrow chimeras were generated by grafting a 1:1 mixture of wild-type (CD45.1) and $Itga4^{\Delta DC}$ (CD45.2) bone marrow into irradiated, matched knockout recipients. After full reconstitution of the peripheral immune compartment, the CNS was analyzed. In this study, we observed an equal distribution of pDCs, cDC1s, and cDC2s in the wild-type and the $Itga4^{\Delta DC}$ compartment in the CNS of mixed bone marrow chimeras both in steady-state (Fig. 1C) and after Flt3L treatment (Fig. 1D). Together, these data indicated that no gross alteration of the CNS DC compartment resulted from genetic ablation of *Itga4* in $CD11c^{+}$ cells.

Disease severity in active EAE is not affected by ablation of Itga4 in myeloid cells

Next, we wanted to test whether constitutive ablation of *Itga4* in DCs had an effect on autoimmune neuroinflammation. In addition to $Itga4^{\Delta DC}$ mice, we ablated *Itga4* in both DCs and monocytes using a combined CD11c Cre and LysM Cre deleter strain. Along with $Itga4^{flox/flox}$ control mice, $Itga4^{\Delta DC}$ mice as well as mice with constitutive ablation of *Itga4* in both DCs and monocytes ($Itga4^{\Delta DC\Delta Mo}$) were immunized with MOG (35–55) in CFA for induction of EAE. Both conditional knockout strains developed clinical disease with similar kinetics and severity as $Itga4^{flox/flox}$ control mice (Fig. 2A). We tested the quantity and the quality of the Ag-specific T cell response in $Itga4^{\Delta DC}$ mice by transferring MOG TCR transgenic reporter cells (2D2) into either control mice ($Itga4^{flox/flox}$) or $Itga4^{\Delta DC}$ mice, followed by immunization with MOG (35–55) in CFA. After 4 d, the proliferation of 2D2 cells reisolated from the draining lymph nodes was similar in control and $Itga4^{\Delta DC}$ mice (Supplemental Fig. 2A), indicating that the priming of Ag-specific T cells in the peripheral immune

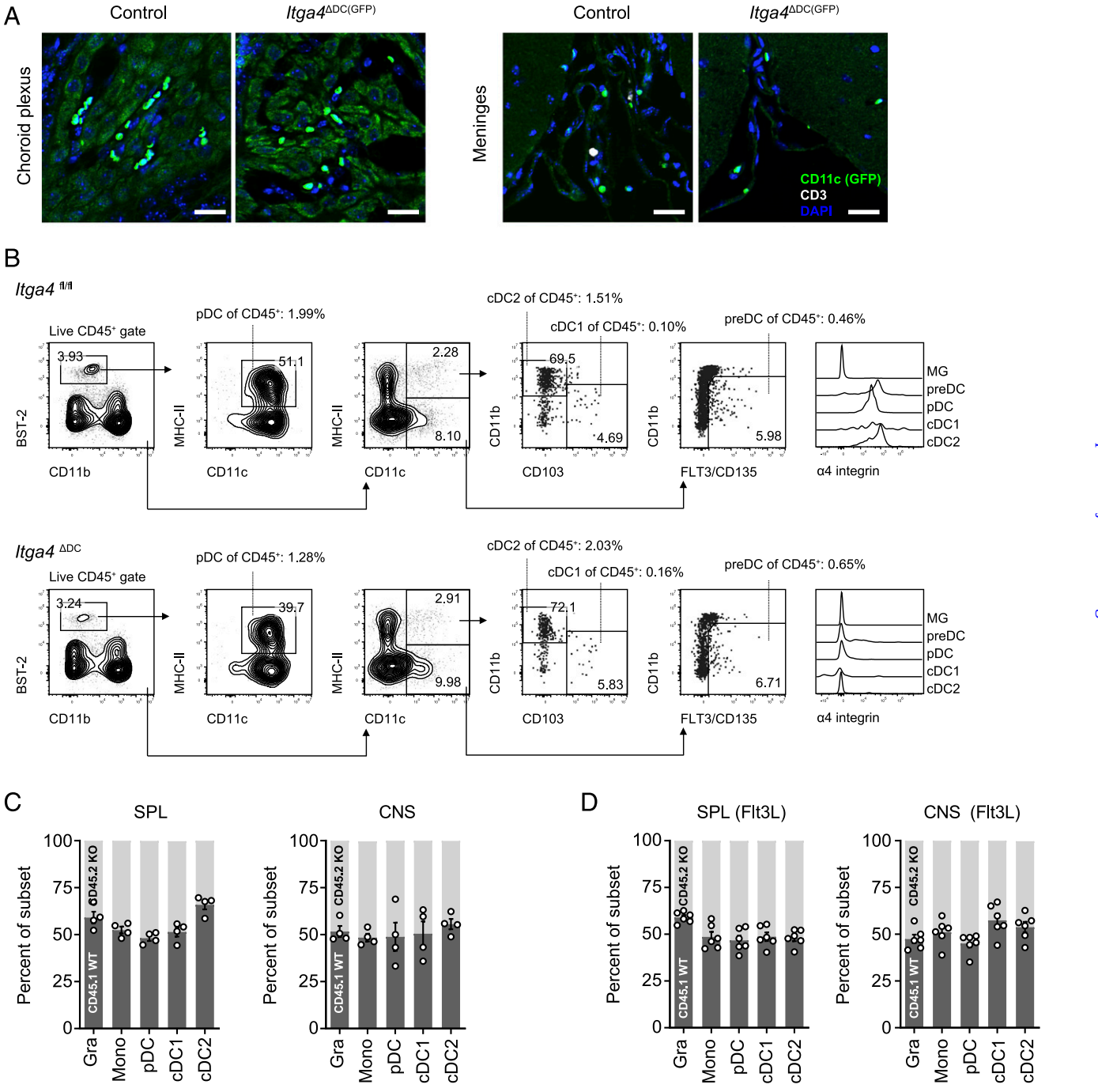

FIGURE 1. DCs accumulate the naive CNS independently of α4 integrin expression. (**A**) Immunofluorescence analysis of brain sections from CD11c-GFP–expressing $Itga4^{\Delta DC(GFP)}$ mice and $Itga4^{flox/WT\ DC(GFP)}$ control littermates. Representative tiles showing choroid plexus and meninges. Scale bar, 20 μm. (**B**) Flow cytometry analysis of the uninflamed total CNS DC compartment from $Itga4^{\Delta DC}$ and $Itga4^{flox/flox}$ littermates. Numbers adjacent to gates indicate parent frequency, overall frequency refers to live $CD45^{high}$ cells. Representative pair of five mice per genotype. Intravascular cells were excluded from analysis by i.v. application of a CD45 staining Ab prior to dissection. Microglia (MG) ($CD45^{int}CD11b^{+}$), pDCs ($BST\text{-}2^{+}CD11b^{-}CD11c^{+}MHC\text{-}II^{+}$), cDC1 ($BST\text{-}2^{-}CD11c^{+}MHC\text{-}II^{+}CD103^{+}CD11b^{low}$) and cDC2 ($BST\text{-}2^{-}CD11c^{+}MHC\text{-}II^{+}CD103^{-}CD11b^{high}$). (**C** and **D**) Chimerism between CD45.2 $Itga4^{\Delta DC}$ and CD45.1 $Itga4^{WT/WT}$ myeloid cells ($CD45^{high}$) in the uninflamed spleen (SPL) and CNS of mixed bone marrow chimeras 8 wk after reconstitution (mean ± SEM). Granulocytes (Gra) ($Ly\text{-}6G^{+}CD11b^{+}B220^{-}CD11c^{-}$), monocytes (Mono) ($MHC\text{-}II^{-}CD11c^{-}CD11b^{+}Ly\text{-}6G^{-}$), pDCs ($MHC\text{-}II^{+}Siglec\text{-}H^{+}BST\text{-}2^{+}B220^{+}CD11c^{+}$), and conventional DCs ($MHC\text{-}II^{+}CD11c^{+}Siglec\text{-}H^{-}BST\text{-}2^{-}B220^{-}$) as cDC1 ($CD103^{+}CD11b^{low}$) and cDC2 ($CD103^{-}CD11b^{high}$). (C) Chimerism in untreated mice, pooled data from four independent experiments. (D) Chimerism 7 d after s.c. injection of 5×10^{6} Flt3L-secreting B16 melanoma cells, pooled data from two independent experiments. Difference to the reference population (Gra) was assessed using Dunnett multiple comparisons test after one-way ANOVA.

compartment was unaltered in $Itga4^{\Delta DC}$ mice upon active immunization with MOG (35–55) in CFA. The identical course of disease in control mice and $Itga4^{\Delta DC}$ mice already suggested that the restimulation of encephalitogenic T cells within the CNS compartment was not impaired. Indeed, we did not observe relevant differences either in the fraction of $Foxp3^{+}$ Treg cells (Supplemental Fig. 2B) or in the profile of effector cytokines in $CD4^{+}$ T cells isolated from the CNS of control mice,

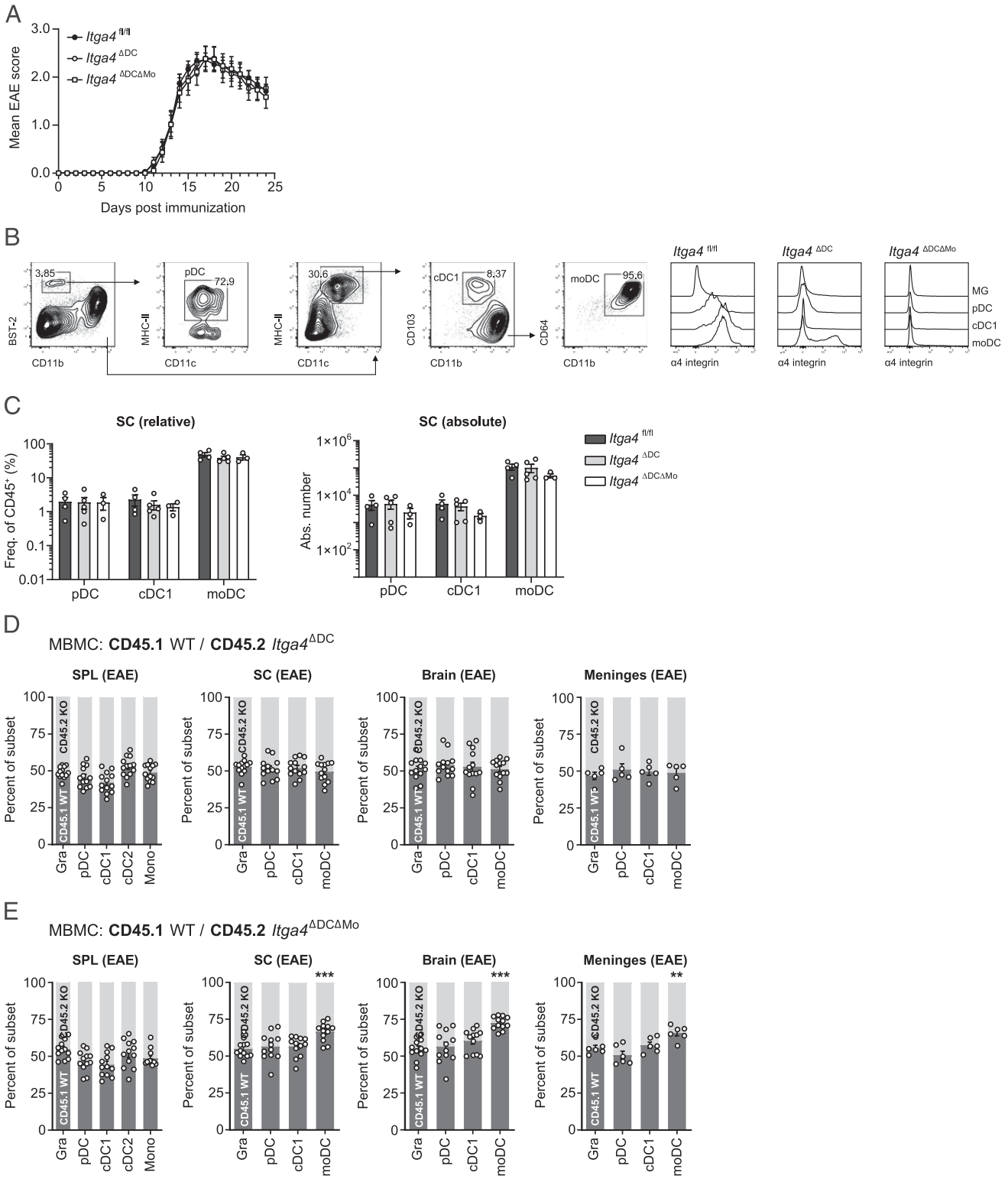

FIGURE 2. α4 integrins on DC are dispensable for active induction of EAE. (**A**) EAE disease course in *Itga4*$^{\Delta DC}$, *Itga4*$^{\Delta DC\Delta Mo}$, and *Itga4*$^{flox/flox}$ control littermates after active immunization with MOG (35–55) in CFA and i.v. PTX administration (mean ± SEM). Pooled data from four independent experiments. Groups were statistically compared on a per-day basis using a one-way ANOVA, followed by Dunnett multiple comparison test. (**B**) Gating strategy and *Itga4* ablation efficiency in myeloid cells of the CNS as measured by flow cytometry at peak disease of active EAE. Microglia (MG) (CD45^{int}CD11b^{+}), pDC (MHC-II^{+}CD11c^{+}BST-2^{+}CD11b^{-}), cDC1 (MHC-II^{+}CD11c^{+}BST-2^{-}CD64^{-}CD11b^{int}CD103^{+}), and moDCs (MHC-II^{+}CD64^{+}CD11b^{+}). (**C**) Relative fraction and absolute number of myeloid cells in spinal cords (SC) of *Itga4*$^{\Delta DC}$ mice, *Itga4*$^{\Delta DC\Delta Mo}$ mice, and *Itga4*$^{flox/flox}$ control littermates at EAE peak disease, as measured by flow cytometry (mean ± SEM). Representative example from four independent experiments with a total number of at least 10 mice per genotype. Groups were statistically compared using a two-way ANOVA, followed by Sidak multiple comparisons test. (**D** and **E**) Chimerism between CD45.2 *Itga4*$^{\Delta DC}$ (D) or CD45.2 *Itga4*$^{\Delta DC\Delta Mo}$ (E) and CD45.1 Itga4$^{WT/WT}$ myeloid cells in the indicated tissues of mixed bone marrow chimeric EAE mice at peak disease (mean ± SEM). Pooled data from four independent experiments. Statistically significant differences in comparison with the control population granulocytes (Gra) (MHC-II^{-}CD11b^{+}CD64^{-}CD11c^{-}BST-2^{-}Ly-6C^{+}Ly-6G^{+}) are reported for each organ according to Dunnett multiple comparison post hoc test following overall significant difference in one-way ANOVA (multiplicity adjusted p values). $^{**}p < 0.01$, $^{***}p < 0.001$. MBMC, ratios of mixed bone marrow chimerism; SPL, spleen.

Itga4$^{\Delta DC}$ mice, or *Itga4*$^{\Delta DC\Delta Mo}$ mice at the peak of EAE (Supplemental Fig. 2C).

To exclude an alteration of the APC composition that is only functionally redundant with regard to downstream T cell effects, we analyzed the DC compartment in the inflamed CNS of control mice as compared with *Itga4*$^{\Delta DC}$ mice or *Itga4*$^{\Delta DC\Delta Mo}$ mice in detail. During inflammation, our gating strategy allowed for the differentiation of pDCs and cDC1s (Fig. 2B). In contrast to steady-state, where, essentially, no monocyte-derived DCs (moDCs) were detected in the CNS (Supplemental Fig. 2D), cDC2s could no longer be unequivocally distinguished from moDCs in EAE, both expressing high levels of CD64 under inflammatory conditions. CNS-derived cDC1s did not express CD64 and were Irf8$^+$, whereas moDCs lacked Irf8 (Supplemental Fig. 2E). *Itga4* was efficiently ablated in pDCs and cDC1s in *Itga4*$^{\Delta DC}$ mice, whereas moDCs were partly spared from *Itga4* ablation (Fig. 2B). Notably, *Itga4* ablation was highly efficient in all DC subsets, including pDCs, cDC1s, and moDCs in *Itga4*$^{\Delta DC\Delta Mo}$ mice (Fig. 2B). In contrast to DC subsets, CD11b$^+$CD45^{int} microglial cells did not express α4 integrins (Fig. 2B). The fractions and absolute numbers of pDCs, cDC1s, and moDCs in the inflamed spinal cord, brain, and meninges of EAE mice were similar in *Itga4*$^{\Delta DC}$ mice and *Itga4*$^{\Delta DC\Delta Mo}$ mice as compared with control animals (Fig. 2C, Supplemental Fig. 2F), suggesting that lack of α4 integrin expression can be compensated as to the recruitment of DC subsets into the inflamed CNS. Of note, the lack of differences in moDC infiltration was not due to a lack of deletional efficiency in progenitors [as reported for the LysM Cre deleter strain in the context of other floxed alleles (39)], because inflammatory monocyte progenitors in the blood postimmunization already exhibited efficient and functional deletion of the floxed α4 allele in *Itga4*$^{\Delta DC\Delta Mo}$ mice prior to infiltrating the CNS (Supplemental Fig. 2G).

LFA-1, an αLβ2 integrin heterodimer, had previously been reported to be dispensable for the recruitment of endogenous myeloid cells in adoptive transfer EAE (40–42). In this study, we asked whether, in the absence of α4 integrin expression on DCs, LFA-1 might become nonredundant for the accumulation of DCs in the CNS during EAE. However, when we blocked LFA-1 with a mAb to CD11a in *Itga4*$^{\Delta DC}$ mice as of day 5 after immunization with MOG (35–55), we failed to protect the mice from clinical disease, and the fractions and numbers of DC subsets in the CNS of anti-CD11a–treated *Itga4*$^{\Delta DC}$ mice were similar to control-treated *Itga4*$^{\Delta DC}$ mice (Supplemental Fig. 2H), suggesting that LFA-1 was irrelevant for the CNS recruitment of α4 integrin–deficient DCs.

Next, we wanted to test the significance of α4 integrins in CD11c$^+$ cells in a competitive setting during inflammation. Again, we constructed bone marrow chimeras and grafted congenically marked wild-type bone marrow (CD45.1$^+$) together with either *Itga4*$^{\Delta DC}$ bone marrow (CD45.2) or *Itga4*$^{\Delta DC\Delta Mo}$ bone marrow (CD45.2) into recipient mice and subjected them to EAE. Consistent with the clinical data, CD11c$^+$ cells deficient in α4 integrins did not show an impaired seeding of the CNS niche during inflammation, even in direct competition with their wild-type counterparts (Fig. 2D). In contrast, lack of α4 integrin expression on moDCs (in the *Itga4*$^{\Delta DC\Delta Mo}$ APC compartment) rendered CD11c$^+$CD11b$^+$ moDCs less fit than their α4 integrin–sufficient counterparts in populating the CNS during inflammation (Fig. 2E). Together, these data suggested that, despite the partial requirement of α4 integrins for the recruitment of moDCs into the CNS, α4 integrin expression on bona fide pDCs and cDCs was dispensable for establishing a functional Ag-presenting compartment in the CNS for full activation of autoreactive T cells in situ.

In situ restimulation of encephalitogenic T cells is fully functional in Itga4$^{\Delta DC}$ mice

To more specifically probe the APC capacity of the CNS in our various α4 integrin–deficient strains, we performed adoptive transfer of exogenously primed Th17 cells into either *Itga4*$^{flox/flox}$ control mice, *Itga4*$^{\Delta DC}$, or *Itga4*$^{\Delta DC\Delta Mo}$ mice. Again, prevalence, kinetics, and severity of adoptive transfer EAE in the knockout strains were similar to those in control recipients (Fig. 3A). Neither did we notice any significant difference in the fractions or absolute numbers of spinal cord– or brain-derived pDCs, cDCs, or moDCs (Fig. 3B, Supplemental Fig. 3A) or in the fraction of Foxp3$^+$ Treg cells or in the profile of effector cytokines of CD4$^+$ T cells reisolated from the CNS (Supplemental Fig. 3B, 3C) of *Itga4*$^{\Delta DC}$ or *Itga4*$^{\Delta DC\Delta Mo}$ mice, as compared with control recipients at the peak of adoptive transfer EAE. In summary, our data indicated that lack of α4 integrins in the DC compartment did not abrogate or even impair the competence of the intrathecal APC compartment to induce and maintain Ag-specific T cell responses.

CD11b$^+$CD103$^+$ DCs are reduced in the lamina propria of Itga4$^{\Delta DC}$ mice

α4 integrins are key homing molecules for immune cells into the gut lamina propria (43). Therefore, we asked whether the gut DC compartment was changed in *Itga4*$^{\Delta DC}$ mice, in which all bona fide DC populations exhibited efficient deletion of α4 integrin (Supplemental Fig. 4A). In steady-state, we found decreased fractions of CD103$^+$CD11b$^+$ double-positive DCs and increased fractions of CD103$^+$CD11b$^-$ single-positive DCs in the small intestinal as well as in the colonic lamina propria of *Itga4*$^{\Delta DC}$ mice, as compared with *Itga4*$^{flox/flox}$ control mice (Fig. 4A), suggesting that double-positive DCs were most dependent on α4 integrins for populating the intestinal lamina propria. In a competitive setting of mixed bone marrow chimeras that had received a 1:1 mixture of wild-type (CD45.1) and *Itga4*$^{\Delta DC}$ (CD45.2) bone marrow, the distribution of all wild-type and *Itga4*$^{\Delta DC}$ DC subsets was even in the spleen (Fig. 1C) but shifted in favor of wild-type DCs, in particular in the CD103$^+$CD11b$^+$ double-positive cDC compartment in the small intestinal and colonic lamina propria, but not in the mesenteric lymph nodes (Fig. 4B). Thus, α4 integrins were required for the accumulation of double-positive DCs in the gut lamina propria.

α4 integrins in DCs are dispensable for host defense against C. rodentium

In the gut, double-positive DCs were proposed to be required for both, the induction of peripherally induced Treg (pTreg) cells that contribute in maintaining immune tolerance against commensal gut bacteria, as well as the priming of protective Th17 responses against pathogens and pathobionts. First, we tested the frequencies of pTreg cells in the gut that are characterized by the coexpression of Foxp3 and RORγt (44) in steady-state. We noticed a slight tendency toward lower fractions of RORγt$^+$Helios$^-$ Treg cells in the small intestinal lamina propria of *Itga4*$^{\Delta DC}$ mice as compared with *Itga4*$^{flox/flox}$ control animals (Supplemental Fig. 4B).

Next, we assessed acute inflammatory responses in the gut in response to i.p. injection of an activating Ab to CD3 (45), which has been shown to induce Th17 responses in the small intestine. The clinical phenotype (weight loss, Fig. 5A) was similar in wild-type littermate controls and *Itga4*$^{\Delta DC}$ mice. These data indicated that the priming of Th17 cells [which have been shown to drive the pathology in this model (45)], can occur with residual amounts of double-positive DCs. Finally, we investigated *C. rodentium* infection, an infectious disease model, which is, in part, dependent on Ag-specific Th17 cells (46). Upon *C. rodentium* infection,

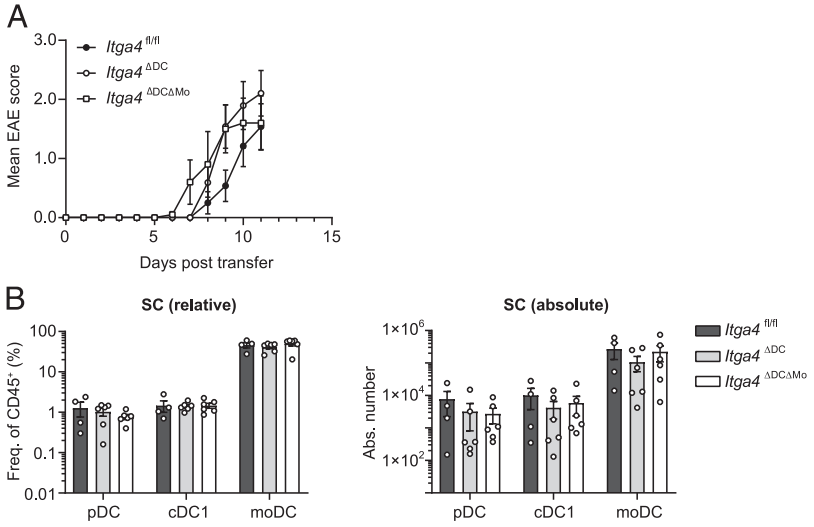

FIGURE 3. *Itga4*$^{\Delta DC}$ mice are fully competent in restimulating encephalitogenic T cells within the CNS compartment. (**A**) Disease course in *Itga4*$^{\Delta DC}$ mice, *Itga4*$^{\Delta DC\Delta Mo}$ mice, and *Itga4*$^{flox/flox}$ littermate control mice following i.v. transfer of 5×10^6 MACS-enriched, CD4$^+$ T cells that had been cultured for 23 d under Th17 skewing conditions (TGF-β, IL-6, and IL-23) in the presence of MOG (35–55) and isolated from wild-type donors 7 d after immunization with MOG (35–55) in CFA. Pooled data from three independent experiments (mean ± SEM). Groups were statistically compared on a per-day basis using a one-way ANOVA, followed by Dunnett multiple comparison test. (**B**) Relative fraction and absolute number of myeloid cells in the spinal cord (SC) of *Itga4*$^{\Delta DC}$, *Itga4*$^{\Delta DC\Delta Mo}$, and *Itga4*$^{flox/flox}$ recipients of encephalitogenic T cells at adoptive transfer EAE peak disease, as measured by flow cytometry (mean ± SEM). pDC (BST-2$^+$CD11b$^-$CD11c$^+$), cDC1 (BST-2$^-$CD11c$^+$CD11b^{int}CD103$^+$), and moDC (CD64$^+$CD11b$^+$). Pooled data from five independent experiments. Groups were statistically compared using a two-way ANOVA, followed by Sidak multiple comparisons test.

wild-type and *Itga4*$^{\Delta DC}$ mice cleared the pathogen equally well (Fig. 5B, 5C). Consistent with the clinical observation, the clear reduction of double-positive cDCs in the lamina propria of the colon that was eminent in steady-state was entirely recovered in inflammation (Fig. 5D), again suggesting that redundant mechanisms can compensate for the lack of α4 integrins on DCs as to their recruitment to sites of inflammation. In summary, the altered DC compartment in *Itga4*$^{\Delta DC}$ mice in the gut did not translate into gross changes of resilience to inflammatory or infectious perturbations, at least in the tested disease models.

Discussion

In this study, we tested the requirement of α4 integrin expression on CD11c$^+$ cells for the seeding of CNS and intestinal niches with CD11c$^+$MHC-II^{high} DCs in steady-state and for the recruitment of DCs during autoimmune inflammation of the CNS and host defense in the gut. Whereas the expression of α4 integrins was largely irrelevant for the replenishment of CNS DCs, the gut-specific population of CD11b$^+$CD103$^+$ DCs was diminished in *Itga4*$^{\Delta DC}$ mice. However, in an infection model with attaching and effacing bacteria, the reduction of this DC population in the colonic lamina propria did not result in an adverse outcome as compared with wild-type control animals. Thus, α4 integrin expression on DCs is a redundant feature in the settings addressed in this study. Differences in the composition of DC populations in *Itga4*$^{\Delta DC}$ mice versus control mice in homeostasis were functionally compensated under inflammatory conditions.

CNS DCs are of hematopoietic origin, and compelling evidence indicates that the capacity to present Ag to T cells in vivo is restricted to these CD11c$^+$ cells, whereas microglial cells are unable to present Ags to T cells (3, 9, 10). Moreover, depletion experiments of DCs using the diphtheria toxin receptor system expressed either in CD11c$^+$ or Zbtb46$^+$ cells have provided strong evidence that the physical presence of DCs in the CNS is required for the productive restimulation of incoming autoreactive T cells (47). The CNS niche is seeded with pre-cDCs that then differentiate into distinct DC subsets in situ (15). In line with previous studies (1, 48, 49), in this study, we showed that the steady-state CNS DC compartment consisted of pDCs (BST2$^+$Siglec-H$^+$), CD11b^{low}CD103$^+$ cDC1s, and CD11b$^+$CD103$^-$ cDC2s, but not moDCs. Flt3L application expanded all DC subsets in the CNS but did not change their relative composition, indicating that moDCs [or TNF and inducible NO synthase producing DCs (50) or CD11c$^+$MHC-II$^+$ monocytes], which do not respond to Flt3L-driven expansion (15, 48), did not contribute to the DC compartment in the CNS during homeostasis. Notably, the process of Flt3L-mediated DC expansion in the CNS was independent of α4 integrin expression by DCs. Also, *Itga4* was as efficiently ablated in pre-cDCs as in pDCs, cDC1s, and cDC2s in *Itga4*$^{\Delta DC}$ mice. Thus, it is unlikely that pre-cDCs seed the CNS niche in a VLA-4–dependent manner and only then lose α4 integrin expression in situ. In fact, none of the steady-state DC subsets (including pre-cDCs) depended on α4 integrins to populate the CNS niche, including meninges and choroid plexus, and *Itga4*$^{\Delta DC}$ mice disposed of a fully replete CNS DC niche. Consistent with these results, restimulation of incoming T cells in the CNS compartment was not altered in *Itga4*$^{\Delta DC}$ mice. These results are in line with prior reports that only physical depletion of CD11c$^+$ DCs cells or Zbtb46$^+$ cDCs from the steady-state CNS is associated with impaired local restimulation of autoreactive T cells (47).

In inflammation, VLA-4 expression on pDCs or cDC1s was dispensable for their CNS recruitment because ablation of *Itga4* did not put CD11c$^+$ cells at a disadvantage to migrate to the inflamed CNS as compared with their wild-type counterparts. CD11c Cre mice showed a complete recombination and thus total loss of α4 integrin expression in all DC subsets. As has been reported before, CD11c Cre resulted in partial ablation of the floxed allele in lymphoid cells as well. However, the α4 integrin mosaic in T cells of *Itga4*$^{\Delta DC}$ mice was functionally irrelevant because wild-type T cells and T cells from *Itga4*$^{\Delta DC}$ mice behaved in an identical manner during EAE. We did not observe any signs of atypical EAE in *Itga4*$^{\Delta DC}$ mice, a phenotype that has been reported in T cell conditional α4 integrin–deficient mice (51).

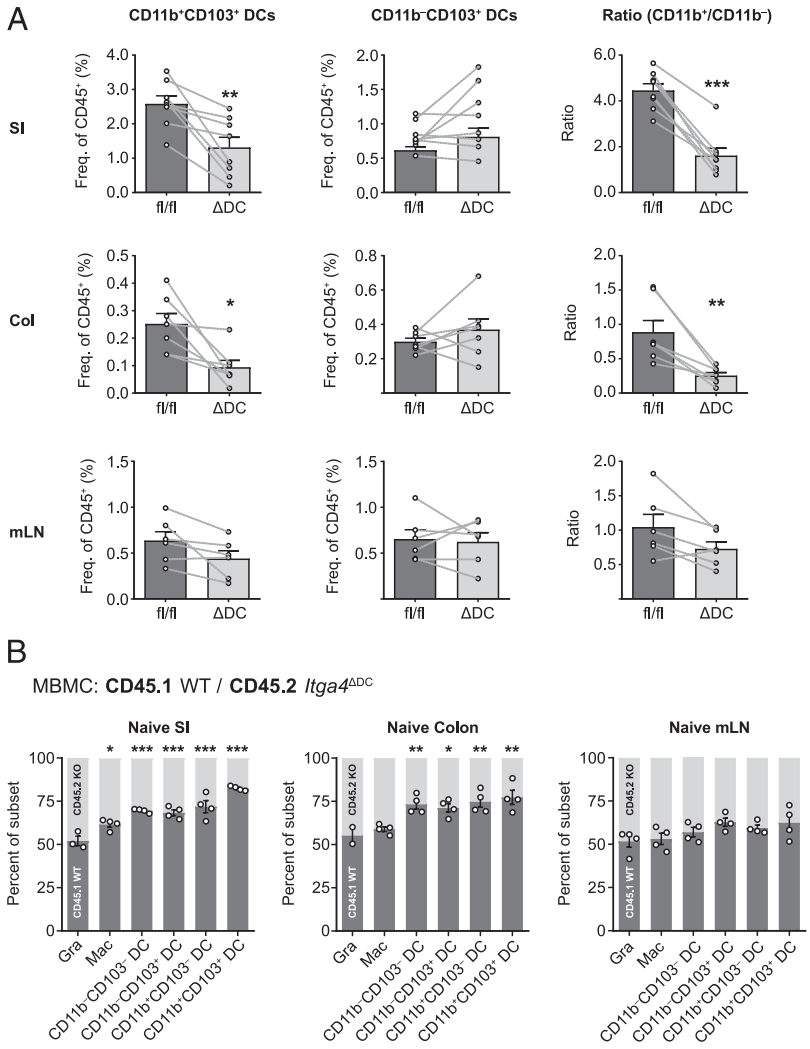

FIGURE 4. Steady-state accumulation of $CD11b^+CD103^+$ DCs in the gut lamina propria is dependent on α4 integrin expression. (**A**) Relative fractions and ratio of $CD11b^+$ and $CD11b^-$ subsets of the $CD103^+$ DC population ($MHC\text{-}II^+CD64^-CD11c^+CD103^+$) in small intestine (SI), colon (Col), and mesenteric lymph nodes (mLN) of naive $Itga4^{\Delta DC}$ mice and $Itga4^{flox/flox}$ littermate controls, as determined by flow cytometry (mean ± SEM). Connecting lines indicate sex-matched, cohoused littermates analyzed on the same day. Pooled data from at least five independent experiments shown. Statistical significance reported from paired two-tailed *t* tests. $*p < 0.05$, $**p < 0.01$, $***p < 0.001$. (**B**) Chimerism between CD45.2 $Itga4^{\Delta DC}$ and CD45.1 $Itga4^{WT/WT}$ myeloid cells in the indicated organs of naive mixed bone marrow chimeric mice (mean ± SEM). Pooled data from two independent experiments. Statistically significant differences as compared with the control population granulocytes (Gra) ($SSC^{high}Ly\text{-}6G^+CD3e^-$) are shown for each organ according to Dunnett multiple comparison post hoc test following overall significant difference in one-way ANOVA (multiplicity adjusted *p* values). $*p < 0.05$, $**p < 0.01$, $***p < 0.001$. MBMC, ratios of mixed bone marrow chimerism.

Interestingly, moDCs depended (at least in part) on the expression of α4 integrins for their recruitment into the inflamed CNS when wild-type and α4 integrin–deficient moDCs competed with each other for the CNS niche in chimeras reconstituted with wild-type plus $Itga4^{\Delta DC\Delta Mo}$ mixed bone marrow. MoDCs are the major effector cells during EAE, are expanded and shaped by GM-CSF, and guided to the CNS in a CCR2-dependent manner (39, 52, 53). However, the α4 integrin–dependent recruitment of moDCs to the CNS was redundant and was overcome during inflammation in $Itga4^{\Delta DC\Delta Mo}$ mice in a noncompetitive setting. In line with these results, a previous report suggested that expression of β1 integrin, the partner of α4 integrin to form heterodimeric VLA-4, was dispensable for the recruitment of myeloid cells into the inflamed CNS (54). Yet, later work suggested that immature DCs need α4 integrins to home to the CNS meningeal space and white matter parenchyma (13). Whereas these conclusions are based on bone marrow–derived DCs that were either deficient in β1 integrin or exposed to anti–VLA-4 Abs in vitro prior to adoptive transfer into host mice with EAE, in this study, we show by genetic ablation of *Itga4* in DCs that endogenous DCs can still migrate into the CNS in the absence of α4 integrin expression. Interestingly, LFA-1 has been reported to be dispensable for the recruitment of myeloid cells into the CNS in adoptive transfer EAE (40–42), whereas, in *Toxoplasma* infection, Ab blockade of LFA-1 reduced the accumulation of adoptively transferred DCs in the CNS (14). In this study, we provided evidence that LFA-1 failed to become a nonredundant mediator of DC recruitment during EAE of $Itga4^{\Delta DC}$ mice. Thus, DCs accumulated in the inflamed CNS despite simultaneous dysfunction of the VLA-4/VCAM1 and LFA-1/ICAM1 pathways, suggesting that the requirements for DC recruitment to the CNS in autoimmunity may differ from T cell recruitment (51) and rely on alternative integrin interactions.

Our data enable a more informed interpretation of the finding that the amount of DCs in the perivascular space of natalizumab treated multiple sclerosis patients was reduced (25). A long-term failure of immune surveillance of the CNS had been proposed because the lack of APCs in the perivascular space would no longer license incoming T cells to patrol the CNS parenchyma. Our observation that DCs are not crucially dependent on α4 integrins for their accumulation in the perivascular and meningeal compartments now suggests that the prolonged depletion of the CNS perivascular space of DCs in natalizumab treated patients is not a direct effect of α4 integrin blockade on DCs. Either the turnover of DCs in the perivascular space is very low, as has been previously suggested in mouse models (11), or (by prior treatment with natalizumab) intrinsic properties of the perivascular niche are changed that would prevent the migration and replenishment of DCs.

Contrary to the CNS compartment, the expression of α4 integrins by $CD11b^+CD103^+$ DCs is required for their maintenance in the lamina propria of the intestine, yet less in the mesenteric lymph nodes. In the gut, $CD11b^+CD103^+$ DCs are Irf4 dependent (21) and are required for the induction of microbiota-specific pTreg cells in the lamina propria and mesenteric lymph

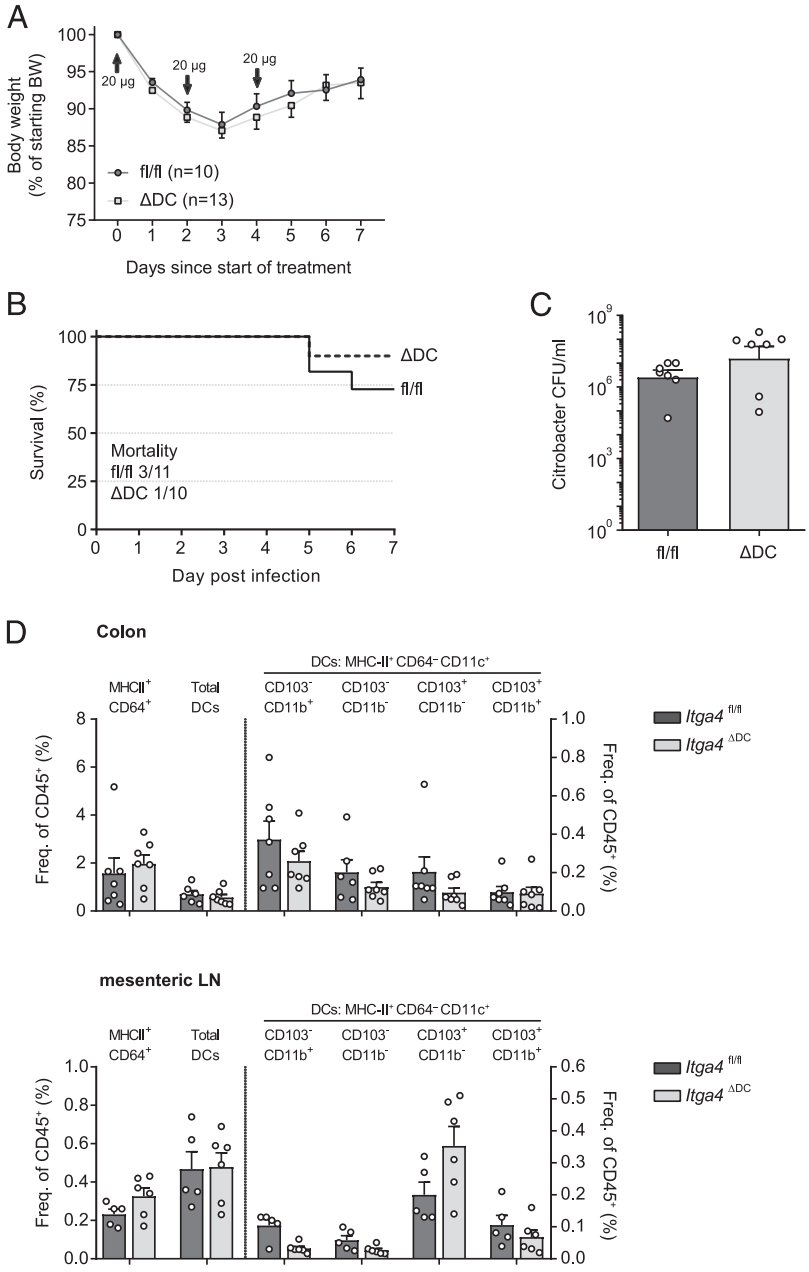

FIGURE 5. Effector T cell priming and host defense in the gut is not dependent on α4 integrin expression by DCs. (**A**) Relative body weight loss of *Itga4*$^{\Delta DC}$ mice and *Itga4*$^{flox/flox}$ littermates following repetitive i.p. injection of 20 μg anti-CD3 Ab as indicated. Groups were compared statistically using two-way ANOVA, followed by Sidak multiple comparisons test. Representative experiment with at least 10 mice per genotype shown (mean ± SEM). (**B**) Survival curve of *Itga4*$^{\Delta DC}$ mice and *Itga4*$^{flox/flox}$ littermate control mice infected with *C. rodentium*. Groups were statistically compared using a log-rank (Mantel–Cox) test. (**C**) Bacterial load in feces derived from colon and cecum of *Citrobacter*-infected *Itga4*$^{\Delta DC}$ mice and *Itga4*$^{flox/flox}$ littermates on day 7 postinfection (mean ± SEM). Groups were statistically compared using a two-tailed, unpaired Student *t* test. (**D**) Relative fraction of myeloid cells in the colon and mesenteric lymph nodes of *Itga4*$^{\Delta DC}$ mice and *Itga4*$^{flox/flox}$ littermate control mice infected with *C. rodentium*, as analyzed by flow cytometry 7 d postinfection (mean ± SEM). Groups were compared using a one-way ANOVA followed by Sidak multiple comparisons test.

nodes (55–57) and the priming of Th17 responses in mesenteric lymph nodes (58). Because, in steady-state, ablation of *Itga4* on CD11c$^+$ cells led to a reduced number (but not complete absence) of CD11b$^+$CD103$^+$ DCs in the lamina propria, the fraction of RORγt$^+$ Treg cells was reduced but not to an extent that resulted in dysbiosis and overt clinical colitis in *Itga4*$^{\Delta DC}$ mice. Our data are in line with the idea that β7 integrins are required for the recruitment of CD11b$^+$CD103$^+$ DCs to the lamina propria (59) and would support the notion that the α4β7 integrin cooperates with the αEβ7 integrin to guide CD11b$^+$CD103$^+$ DCs to the lamina propria, where these DCs are involved in the induction of pTreg cells. However, long-term observation of *Itga4*$^{\Delta DC}$ mice will be required to further address this question. Conversely, Ag presentation by CD11b$^+$CD103$^+$ DCs in the mesenteric lymph node appeared to be intact in *Itga4*$^{\Delta DC}$ mice because robust *C. rodentium*–specific Th17 responses were raised in *Itga4*$^{\Delta DC}$ mice. Indeed, CD11b$^+$CD103$^+$ DCs in the mesenteric lymph nodes were proposed to be the nonredundant source of IL-23 in response to *C. rodentium*–derived flagellin to induce IL-22 in innate lymphoid cells (60) and to prime Th17 responses (58). In steady-state, CD11b$^+$CD103$^+$ DCs had a disadvantage in populating the small intestinal and colonic lamina propria as compared with their α4 integrin–sufficient competitors. However, in inflammation (both upon anti-CD3 injection and in *C. rodentium* infection), the recruitment of DCs into the lamina propria and their trafficking to the mesenteric lymph nodes were not obviously impaired in *Itga4*$^{\Delta DC}$ mice. Although *Itga4*$^{\Delta DC}$ mice were able to clear a primary *C. rodentium* infection, it is possible that the relative reduction of CD11b$^+$CD103$^+$ DCs in the lamina propria of *Itga4*$^{\Delta DC}$ mice affected the generation of *C. rodentium*–specific memory T cells with potential consequences for recall responses. Further studies are required to investigate this question in detail.

In conclusion, in this study, we definitively show that DC recruitment in the CNS occurs independently of α4 integrin expression both in tissue homeostasis and under inflammatory conditions. Although the DC population in the lamina propria is perturbed in *Itga4*$^{\Delta DC}$ mice, functional consequences for autoimmunity or host defense do not emanate from this altered DC

compartment. Our study illustrates that targeting α4 integrins may not be an efficient means in modulating local APC compartments in the gut and CNS. In particular in the CNS, the tissue-specific APC competence is believed to correlate with compartmentalized inflammatory processes during the progressive phase of autoimmune neuroinflammation (in multiple sclerosis) and has been identified as a potential therapeutic target to control tissue restricted chronic inflammation. However, we now provide evidence that other targets than α4 integrins might be more appropriate in resetting the APC competence of nonlymphoid tissues during prolonged inflammation.

Acknowledgments

We thank Veronika Husterer and Svenja Bourry for skillful technical assistance.

Disclosures

The authors have no financial conflicts of interest.

References

1. Prodinger, C., J. Bunse, M. Krüger, F. Schiefenhövel, C. Brandt, J. D. Laman, M. Greter, K. Immig, F. Heppner, B. Becher, and I. Bechmann. 2011. CD11c-expressing cells reside in the juxtavascular parenchyma and extend processes into the glia limitans of the mouse nervous system. *Acta Neuropathol.* 121: 445–458.
2. Bulloch, K., M. M. Miller, J. Gal-Toth, T. A. Milner, A. Gottfried-Blackmore, E. M. Waters, U. W. Kaunzner, K. Liu, R. Lindquist, M. C. Nussenzweig, et al. 2008. CD11c/EYFP transgene illuminates a discrete network of dendritic cells within the embryonic, neonatal, adult, and injured mouse brain. *J. Comp. Neurol.* 508: 687–710.
3. Hickey, W. F., and H. Kimura. 1988. Perivascular microglial cells of the CNS are bone marrow-derived and present antigen in vivo. *Science* 239: 290–292.
4. Kierdorf, K., D. Erny, T. Goldmann, V. Sander, C. Schulz, E. G. Perdiguero, P. Wieghofer, A. Heinrich, P. Riemke, C. Hölscher, et al. 2013. Microglia emerge from erythromyeloid precursors via Pu.1- and Irf8-dependent pathways. *Nat. Neurosci.* 16: 273–280.
5. Ginhoux, F., M. Greter, M. Leboeuf, S. Nandi, P. See, S. Gokhan, M. F. Mehler, S. J. Conway, L. G. Ng, E. R. Stanley, et al. 2010. Fate mapping analysis reveals that adult microglia derive from primitive macrophages. *Science* 330: 841–845.
6. Schulz, C., E. Gomez Perdiguero, L. Chorro, H. Szabo-Rogers, N. Cagnard, K. Kierdorf, M. Prinz, B. Wu, S. E. W. Jacobsen, J. W. Pollard, et al. 2012. A lineage of myeloid cells independent of Myb and hematopoietic stem cells. *Science* 336: 86–90.
7. Greter, M., F. L. Heppner, M. P. Lemos, B. M. Odermatt, N. Goebels, T. Laufer, R. J. Noelle, and B. Becher. 2005. Dendritic cells permit immune invasion of the CNS in an animal model of multiple sclerosis. *Nat. Med.* 11: 328–334.
8. Immig, K., M. Gericke, F. Menzel, F. Merz, M. Krueger, F. Schiefenhövel, A. Lösche, K. Jäger, U.-K. Hanisch, K. Biber, and I. Bechmann. 2015. CD11c-positive cells from brain, spleen, lung, and liver exhibit site-specific immune phenotypes and plastically adapt to new environments. *Glia* 63: 611–625.
9. Mundt, S., D. Mrdjen, S. G. Utz, M. Greter, B. Schreiner, and B. Becher. 2019. Conventional DCs sample and present myelin antigens in the healthy CNS and allow parenchymal T cell entry to initiate neuroinflammation. *Sci. Immunol.* 4: eaau8380.
10. Jordão, M. J. C., R. Sankowski, S. M. Brendecke, G. Sagar, G. Locatelli, Y. H. Tai, T. L. Tay, E. Schramm, S. Armbruster, N. Hagemeyer, et al. 2019. Single-cell profiling identifies myeloid cell subsets with distinct fates during neuroinflammation. *Science* 363: eaat7554.
11. Goldmann, T., P. Wieghofer, M. J. C. Jordão, F. Prutek, N. Hagemeyer, K. Frenzel, L. Amann, O. Staszewski, K. Kierdorf, M. Krueger, et al. 2016. Origin, fate and dynamics of macrophages at central nervous system interfaces. *Nat. Immunol.* 17: 797–805.
12. Mrdjen, D., A. Pavlovic, F. J. Hartmann, B. Schreiner, S. G. Utz, B. P. Leung, I. Lelios, F. L. Heppner, J. Kipnis, D. Merkler, et al. 2018. High-dimensional single-cell mapping of central nervous system immune cells reveals distinct myeloid subsets in health, aging, and disease. [Published erratum appears in 2018 *Immunity* 48: 599.] *Immunity* 48: 380–395.e6.
13. Jain, P., C. Coisne, G. Enzmann, R. Rottapel, and B. Engelhardt. 2010. Alpha4beta1 integrin mediates the recruitment of immature dendritic cells across the blood-brain barrier during experimental autoimmune encephalomyelitis. *J. Immunol.* 184: 7196–7206.
14. John, B., B. Ricart, E. D. Tait Wojno, T. H. Harris, L. M. Randall, D. A. Christian, B. Gregg, D. M. De Almeida, W. Weninger, D. A. Hammer, and C. A. Hunter. 2011. Analysis of behavior and trafficking of dendritic cells within the brain during toxoplasmic encephalitis. *PLoS Pathog.* 7: e1002246.
15. Anandasabapathy, N., G. D. Victora, M. Meredith, R. Feder, B. Dong, C. Kluger, K. Yao, M. L. Dustin, M. C. Nussenzweig, R. M. Steinman, and K. Liu. 2011. Flt3L controls the development of radiosensitive dendritic cells in the meninges and choroid plexus of the steady-state mouse brain. *J. Exp. Med.* 208: 1695–1705.
16. Irla, M., N. Küpfer, T. Suter, R. Lissilaa, M. Benkhoucha, J. Skupsky, P. H. Lalive, A. Fontana, W. Reith, and S. Hugues. 2010. MHC class II-restricted antigen presentation by plasmacytoid dendritic cells inhibits T cell-mediated autoimmunity. *J. Exp. Med.* 207: 1891–1905.
17. Duraes, F. V., C. Lippens, K. Steinbach, J. Dubrot, D. Brighouse, N. Bendriss-Vermare, S. Issazadeh-Navikas, D. Merkler, and S. Hugues. 2016. pDC therapy induces recovery from EAE by recruiting endogenous pDC to sites of CNS inflammation. *J. Autoimmun.* 67: 8–18.
18. Isaksson, M., B. Ardesjö, L. Rönnblom, O. Kämpe, H. Lassmann, M.-L. Eloranta, and A. Lobell. 2009. Plasmacytoid DC promote priming of autoimmune Th17 cells and EAE. *Eur. J. Immunol.* 39: 2925–2935.
19. Sie, C., and T. Korn. 2017. Dendritic cells in central nervous system autoimmunity. *Semin. Immunopathol.* 39: 99–111.
20. Briseño, C. G., T. L. Murphy, and K. M. Murphy. 2014. Complementary diversification of dendritic cells and innate lymphoid cells. *Curr. Opin. Immunol.* 29: 69–78.
21. Persson, E. K., H. Uronen-Hansson, M. Semmrich, A. Rivollier, K. Hägerbrand, J. Marsal, S. Gudjonsson, U. Håkansson, B. Reizis, K. Kotarsky, and W. W. Agace. 2013. IRF4 transcription-factor-dependent CD103(+)CD11b(+) dendritic cells drive mucosal T helper 17 cell differentiation. *Immunity* 38: 958–969.
22. del Rio, M.-L., J.-I. Rodriguez-Barbosa, E. Kremmer, and R. Förster. 2007. CD103- and CD103+ bronchial lymph node dendritic cells are specialized in presenting and cross-presenting innocuous antigen to CD4+ and CD8+ T cells. *J. Immunol.* 178: 6861–6866.
23. Bedoui, S., P. G. Whitney, J. Waithman, L. Eidsmo, L. Wakim, I. Caminschi, R. S. Allan, M. Wojtasiak, K. Shortman, F. R. Carbone, et al. 2009. Cross-presentation of viral and self antigens by skin-derived CD103+ dendritic cells. *Nat. Immunol.* 10: 488–495.
24. Hou, B., A. Benson, L. Kuzmich, A. L. DeFranco, and F. Yarovinsky. 2011. Critical coordination of innate immune defense against *Toxoplasma gondii* by dendritic cells responding via their Toll-like receptors. *Proc. Natl. Acad. Sci. USA* 108: 278–283.
25. del Pilar Martin, M., P. D. Cravens, R. Winger, E. M. Frohman, M. K. Racke, T. N. Eagar, S. S. Zamvil, M. S. Weber, B. Hemmer, N. J. Karandikar, et al. 2008. Decrease in the numbers of dendritic cells and CD4+ T cells in cerebral perivascular spaces due to natalizumab. *Arch. Neurol.* 65: 1596–1603.
26. Derfuss, T., J. M. Kovarik, L. Kappos, M. Savelieva, R. Chhabra, A. Thakur, Y. Zhang, H. Wiendl, and D. Tomic. 2017. α4-integrin receptor desaturation and disease activity return after natalizumab cessation. *Neurol. Neuroimmunol. Neuroinflamm.* 4: e388.
27. Stüve, O., C. M. Marra, K. R. Jerome, L. Cook, P. D. Cravens, S. Cepok, E. M. Frohman, J. T. Phillips, G. Arendt, B. Hemmer, et al. 2006. Immune surveillance in multiple sclerosis patients treated with natalizumab. *Ann. Neurol.* 59: 743–747.
28. Bettelli, E., M. Pagany, H. L. Weiner, C. Linington, R. A. Sobel, and V. K. Kuchroo. 2003. Myelin oligodendrocyte glycoprotein-specific T cell receptor transgenic mice develop spontaneous autoimmune optic neuritis. *J. Exp. Med.* 197: 1073–1081.
29. Bettelli, E., Y. Carrier, W. Gao, T. Korn, T. B. Strom, M. Oukka, H. L. Weiner, and V. K. Kuchroo. 2006. Reciprocal developmental pathways for the generation of pathogenic effector TH17 and regulatory T cells. *Nature* 441: 235–238.
30. Scott, L. M., G. V. Priestley, and T. Papayannopoulou. 2003. Deletion of alpha4 integrins from adult hematopoietic cells reveals roles in homeostasis, regeneration, and homing. *Mol. Cell. Biol.* 23: 9349–9360.
31. Caton, M. L., M. R. Smith-Raska, and B. Reizis. 2007. Notch-RBP-J signaling controls the homeostasis of CD8- dendritic cells in the spleen. *J. Exp. Med.* 204: 1653–1664.
32. Stranges, P. B., J. Watson, C. J. Cooper, C.-M. Choisy-Rossi, A. C. Stonebraker, R. A. Beighton, H. Hartig, J. P. Sundberg, S. Servick, G. Kaufmann, et al. 2007. Elimination of antigen-presenting cells and autoreactive T cells by Fas contributes to prevention of autoimmunity. *Immunity* 26: 629–641.
33. Clausen, B. E., C. Burkhardt, W. Reith, R. Renkawitz, and I. Förster. 1999. Conditional gene targeting in macrophages and granulocytes using LysMcre mice. *Transgenic Res.* 8: 265–277.
34. Korn, T., M. Mitsdoerffer, A. L. Croxford, A. Awasthi, V. A. Dardalhon, G. Galileos, P. Vollmar, G. L. Stritesky, M. H. Kaplan, A. Waisman, et al. 2008. IL-6 controls Th17 immunity in vivo by inhibiting the conversion of conventional T cells into Foxp3+ regulatory T cells. *Proc. Natl. Acad. Sci. USA* 105: 18460–18465.
35. Schlitzer, A., A. F. Heiseke, H. Einwächter, W. Reindl, M. Schiemann, C.-P. Manta, P. See, J. H. Niess, T. Suter, F. Ginhoux, and A. B. Krug. 2012. Tissue-specific differentiation of a circulating CCR9- pDC-like common dendritic cell precursor. *Blood* 119: 6063–6071.
36. Rambaldi, D., S. Pece, and P. P. Di Fiore. 2014. flowFit: a Bioconductor package to estimate proliferation in cell-tracking dye studies. *Bioinformatics* 30: 2060–2065.
37. Abram, C. L., G. L. Roberge, Y. Hu, and C. A. Lowell. 2014. Comparative analysis of the efficiency and specificity of myeloid-Cre deleting strains using ROSA-EYFP reporter mice. *J. Immunol. Methods* 408: 89–100.
38. Baschant, U., L. Frappart, U. Rauchhaus, L. Bruns, H. M. Reichardt, T. Kamradt, R. Bräuer, and J. P. Tuckermann. 2011. Glucocorticoid therapy of antigen-induced arthritis depends on the dimerized glucocorticoid receptor in T cells. *Proc. Natl. Acad. Sci. USA* 108: 19317–19322.
39. Croxford, A. L., M. Lanzinger, F. J. Hartmann, B. Schreiner, F. Mair, P. Pelczar, B. E. Clausen, S. Jung, M. Greter, and B. Becher. 2015. The cytokine GM-CSF drives the inflammatory signature of CCR2+ monocytes and licenses autoimmunity. *Immunity* 43: 502–514.

40. Welsh, C. T., J. W. Rose, K. E. Hill, and J. J. Townsend. 1993. Augmentation of adoptively transferred experimental allergic encephalomyelitis by administration of a monoclonal antibody specific for LFA-1 alpha. *J. Neuroimmunol.* 43: 161–167.
41. Rose, J. W., C. T. Welsh, K. E. Hill, M. K. Houtchens, R. S. Fujinami, and J. J. Townsend. 1999. Contrasting effects of anti-adhesion molecule therapy in experimental allergic encephalomyelitis and Theiler's murine encephalomyelitis. *J. Neuroimmunol.* 97: 110–118.
42. Dugger, K. J., K. R. Zinn, C. Weaver, D. C. Bullard, and S. R. Barnum. 2009. Effector and suppressor roles for LFA-1 during the development of experimental autoimmune encephalomyelitis. *J. Neuroimmunol.* 206: 22–27.
43. Berlin, C., E. L. Berg, M. J. Briskin, D. P. Andrew, P. J. Kilshaw, B. Holzmann, I. L. Weissman, A. Hamann, and E. C. Butcher. 1993. Alpha 4 beta 7 integrin mediates lymphocyte binding to the mucosal vascular addressin MAdCAM-1. *Cell* 74: 185–195.
44. Ohnmacht, C., J.-H. Park, S. Cording, J. B. Wing, K. Atarashi, Y. Obata, V. Gaboriau-Routhiau, R. Marques, S. Dulauroy, M. Fedoseeva, et al. 2015. MUCOSAL IMMUNOLOGY. The microbiota regulates type 2 immunity through RORγt$^+$ T cells. *Science* 349: 989–993.
45. Esplugues, E., S. Huber, N. Gagliani, A. E. Hauser, T. Town, Y. Y. Wan, W. O'Connor, Jr., A. Rongvaux, N. Van Rooijen, A. M. Haberman, et al. 2011. Control of TH17 cells occurs in the small intestine. *Nature* 475: 514–518.
46. Atarashi, K., T. Tanoue, M. Ando, N. Kamada, Y. Nagano, S. Narushima, W. Suda, A. Imaoka, H. Setoyama, T. Nagamori, et al. 2015. Th17 cell induction by adhesion of microbes to intestinal epithelial cells. *Cell* 163: 367–380.
47. Giles, D. A., P. C. Duncker, N. M. Wilkinson, J. M. Washnock-Schmid, and B. M. Segal. 2018. CNS-resident classical DCs play a critical role in CNS autoimmune disease. *J. Clin. Invest.* 128: 5322–5334.
48. Curtin, J. F., G. D. King, C. Barcia, C. Liu, F. X. Hubert, C. Guillonneau, R. Josien, I. Anegon, P. R. Lowenstein, and M. G. Castro. 2006. Fms-like tyrosine kinase 3 ligand recruits plasmacytoid dendritic cells to the brain. *J. Immunol.* 176: 3566–3577.
49. Quintana, E., A. Fernández, P. Velasco, B. de Andrés, I. Liste, D. Sancho, M. L. Gaspar, and E. Cano. 2015. DNGR-1(+) dendritic cells are located in meningeal membrane and choroid plexus of the noninjured brain. *Glia* 63: 2231–2248.
50. Ji, Q., L. Castelli, and J. M. Goverman. 2013. MHC class I-restricted myelin epitopes are cross-presented by Tip-DCs that promote determinant spreading to CD8$^+$ T cells. *Nat. Immunol.* 14: 254–261.
51. Rothhammer, V., S. Heink, F. Petermann, R. Srivastava, M. C. Claussen, B. Hemmer, and T. Korn. 2011. Th17 lymphocytes traffic to the central nervous system independently of α4 integrin expression during EAE. *J. Exp. Med.* 208: 2465–2476.
52. King, I. L., T. L. Dickendesher, and B. M. Segal. 2009. Circulating Ly-6C+ myeloid precursors migrate to the CNS and play a pathogenic role during autoimmune demyelinating disease. *Blood* 113: 3190–3197.
53. Mildner, A., M. Mack, H. Schmidt, W. Brück, M. Djukic, M. D. Zabel, A. Hille, J. Priller, and M. Prinz. 2009. CCR2+Ly-6Chi monocytes are crucial for the effector phase of autoimmunity in the central nervous system. *Brain* 132: 2487–2500.
54. Bauer, M., C. Brakebusch, C. Coisne, M. Sixt, H. Wekerle, B. Engelhardt, and R. Fässler. 2009. Beta1 integrins differentially control extravasation of inflammatory cell subsets into the CNS during autoimmunity. *Proc. Natl. Acad. Sci. USA* 106: 1920–1925.
55. Coombes, J. L., K. R. R. Siddiqui, C. V. Arancibia-Cárcamo, J. Hall, C.-M. Sun, Y. Belkaid, and F. Powrie. 2007. A functionally specialized population of mucosal CD103+ DCs induces Foxp3+ regulatory T cells via a TGF-beta and retinoic acid-dependent mechanism. *J. Exp. Med.* 204: 1757–1764.
56. Lathrop, S. K., S. M. Bloom, S. M. Rao, K. Nutsch, C.-W. Lio, N. Santacruz, D. A. Peterson, T. S. Stappenbeck, and C.-S. Hsieh. 2011. Peripheral education of the immune system by colonic commensal microbiota. *Nature* 478: 250–254.
57. Barthels, C., A. Ogrinc, V. Steyer, S. Meier, F. Simon, M. Wimmer, A. Blutke, T. Straub, U. Zimber-Strobl, E. Lutgens, et al. 2017. CD40-signalling abrogates induction of RORγt$^+$ Treg cells by intestinal CD103$^+$ DCs and causes fatal colitis. *Nat. Commun.* 8: 14715.
58. Satpathy, A. T., C. G. Briseño, J. S. Lee, D. Ng, N. A. Manieri, W. Kc, X. Wu, S. R. Thomas, W.-L. Lee, M. Turkoz, et al. 2013. Notch2-dependent classical dendritic cells orchestrate intestinal immunity to attaching-and-effacing bacterial pathogens. *Nat. Immunol.* 14: 937–948.
59. Villablanca, E. J., J. De Calisto, P. Torregrosa Paredes, B. Cassani, D. D. Nguyen, S. Gabrielsson, and J. R. Mora. 2014. β7 integrins are required to give rise to intestinal mononuclear phagocytes with tolerogenic potential. *Gut* 63: 1431–1440.
60. Kinnebrew, M. A., C. G. Buffie, G. E. Diehl, L. A. Zenewicz, I. Leiner, T. M. Hohl, R. A. Flavell, D. R. Littman, and E. G. Pamer. 2012. Interleukin 23 production by intestinal CD103(+)CD11b(+) dendritic cells in response to bacterial flagellin enhances mucosal innate immune defense. *Immunity* 36: 276–287.